Journal of Electroanalytical Chemistry 897 (2021) 115580

Contents lists available at ScienceDirect

Journal of Electroanalytical Chemistry

journal homepage: www.elsevier.com/locate/jelechem

The role of lithium, perchlorate and water during electrochemical processes in poly(3,4-ethylenedioxythiophene) films in $LiClO_4$ aqueous solutions

E. Guillén, J. Agrisuelas, J.J. García-Jareño *, F. Vicente

Departament de Química Física, Universitat de València. C/Dr. Moliner, 50, Burjassot, València 46100, Spain

ARTICLE INFO

Keywords:
Poly(3,4-ethylenedioxythiophene) (PEDOT)
Ion and solvent doping
vis-NIR spectroelectrochemistry
electrochemical quartz crystal microbalance (EQCM)
Motional Resistance
Lithium exchange

ABSTRACT

Thin films of poly(3,4-ethylendioxythiophene) (PEDOT) were electrochemically deposited on gold electrodes in aqueous media. The role of perchlorate, lithium, and water during the charge/discharge of PEDOT films was investigated by cyclic voltammetry together with EQCM, vis − NIR spectroscopy, and acoustic impedance, also by means of ac-electrogravimetry in a 0.1 M $LiClO_4$ aqueous solutions. In this way, it has been possible to correlate the electrical, mass, color and electromechanical properties changes during the electrochemical reactions of this polymer. Both, hydrated lithium cations and perchlorate anions can act as counterions during the electrochemical reactions, however, at the more positive potentials anions are the preferred ions while at the more negative potentials the relative participation of cations increases. A secondary electrochemical reaction appears in aqueous solutions at potentials near −0.38 V against the Ag|AgCl|KCl(sat) reference electrode and it is neither associated with mass changes nor with spectroscopic changes of the PEDOT. Viscoelastic properties of the film change also with the applied potential and this change is mainly observed at the more negative potentials due to the exchange of highly hydrated Li^+ cations.

1. Introduction

In recent years, poly(3,4-ethylenedioxythiophene) (PEDOT) has become one of the most studied smart polymers due to its good conductivity, processability, stability and their possible use as a material for supercapacitor devices [1-4]. PEDOT has a rigid and linear conformation that facilitates packing and electronic transport involving high and fast charge/discharge processes[5]. These features make PEDOT one of the conducting polymers commercially produced increasingly on large scale lately and sold for a wide variety of applications like sensors[6], anti-static coatings[7], light-emitting devices[8], solar cells [9], supercapacitors[10], actuators[11] and even as a biological tissue interfacing agent[12].

Different authors have studied the mechanism of oxidation/reduction of PEDOT, but with some discrepancy about the role of ions and the effect of the solvent. Hillman et al. and Bull et al. have explained the mechanism for the p-doping [13-16]. In recent studies, Tao Le et al. also study the role of cations in this process [17]. From a molecular perspective, the rearrangement of the polymer by creating or destroying double bonds and by accommodating anions affects the free volume occupied by free solvent molecules within the film [18]. Their redox processes are accompanied by color changes from light blue in the charged form to a dark blue in the neutral form [19] and the reversible transfer of counterions and solvent between the solution and the polymer [20-23]. This knowledge is possible by the *in situ* combination of different techniques during electrochemical processes [24,25]. Among others, spectroelectrochemical and electrogravimetric *in situ* assembled techniques have been successfully used during the last years for the study of electrochemical processes in conducting polymers. This is the case of our laboratory where cyclic voltammetry is coupled with a Vis-NIR spectrometer and a quartz crystal microbalance with motional resistance monitoring (QCM-R) [26,27]. The motional resistance (R_m) is an instantaneous measurement of the real part of the acoustical impedance associated with the Butterworth-Van Dyke equivalent circuit of a resonant electrode[28-35]. Then, the R_m electromechanical magnitude offers information about the viscoelastic properties of the PEDOT/interface system. If the deposited layer is rigid enough, transversal waves lose relatively little energy. On the contrary, viscous layers involve a significant energy loss or the wave damping [34-36]. This change is associated in both cases to the ion and neutral species exchanged. This is key information for the design of new devices based on this material for their use in energy storage devices such as supercapacitors or batteries.

* Corresponding author.
E-mail address: Jose.J.Garcia@uv.es (J.J. García-Jareño).

https://doi.org/10.1016/j.jelechem.2021.115580
Received 23 January 2021; Received in revised form 21 July 2021; Accepted 30 July 2021
Available online 3 August 2021

Both, electron and counterion transport through conducting polymers are coupled. Electron transport has been described as an electron hopping between neighbor active centers in the polymer and the global process as an electron percolation through the material. Counterions insertion and transport are necessary to keep the film electroneutrality and in some cases can be the rate-determining step. EIS has been largely used for interpreting kinetics and charge transport mechanisms in these polymers and in recent years electrogravimetric techniques in the ac-regime (ac-electrogravimetry or mass impedance, $\frac{\Delta m}{\Delta E}(\omega)$) together with EIS ($\frac{\Delta E}{\Delta I}(\omega)$) which allows discerning among the role of anions, cation and solvent and also, between faster and slower processes by the frequencies scan [37-41]. The use of the crossed impedance transfer function $F\Delta m/\Delta q(\omega)$ obtained from EIS and ac-electrogravimetry also allows discerning among different exchanged species by their molar masses [25,27,42]. This function represents the mass/electric charge ratio during an electrochemical experiment and gives an estimation of the weighted mean value of the molar masses of species exchanged during the electrochemical redox process[42-44]:

$$F\left(\frac{\Delta m}{\Delta q}\right)(\omega) = F \cdot A \cdot \left(\frac{\Delta m}{\Delta E}\right)\left(\frac{\Delta E}{j\omega\Delta I}\right) = \sum \nu_i \frac{MW_i}{-z_i} \pm \xi \quad (1)$$

It is similar in the dc-regime, but in this case, Fdm/dq is obtained from mass derivative and current (dq/dt):

$$F\frac{dm}{dq} = F\left(\frac{\frac{dm}{dt}}{\frac{dq}{dt}}\right) = \sum \nu_i \frac{MW_i}{-z_i} \pm \xi \quad (2)$$

where F is the Faraday constant (96485 C mol^{-1}), ξ corresponds to the mass contribution of solvent or non-charged species. MW_i is the molar mass of the i charged species involved in the faradaic process, z_i represents the electrical charge of the ion i that participates in the electrochemical process and ν_i is the associated charge compensated by the participation of each i species [26,27,39,45]. The minus sign appears in this equation since the exchange of cations gives negative values of this function and the opposite for the anions exchange. If some of the electrochemical processes do not involve mass changes, i.e. a chemical/electrochemical reaction of the outer solution, the molecular mass associated with this process should be considered as 0, making the absolute value of Fdm/dq to be smaller than that expected.

It is well known that polymerization conditions determine the electrochemical and morphological properties of PEDOT [46,47]. Usually, PEDOT is electrogenerated in organic media because of the low solubility of the thiophene structures in water, but also because of the oxidation potentials higher than potentials of the oxygen evolution in water and the water-catalyzed formation of thienyl cation radicals, which can activate concomitant reactions and can hinder the formation of the main polymer [48,49]. Despite this, there are some investigations where PEDOT was synthesized in an aqueous solution, using anionic[50,51], cationic[52] and non-ionic surfactants[53], but also without any surfactant [54]. PEDOT films electrosynthetized in aqueous media show excellent electrochromic performances [55] and stability [56]. These studies, although minorities offer a more sustainable and safer alternative synthesis and investigations.

The aim of this work is, on the one hand, to contribute to the knowledge of the mechanisms by which this polymer is electrogenerated on the electrode surface in aqueous media and on the other hand to elucidate the different role of hydrated lithium, perchlorate anions and water molecules during the electrochemical redox reactions. Hyphenated techniques above mentioned give us a wide view of the mechanisms by which these electrochemical processes occur in PEDOT films.

2. Experimental

A typical three electrodes cell was used for the synthesis and characterization of PEDOT films. The auxiliary electrode was a Pt mesh, the reference was the Ag|AgCl|KCl(sat) electrode which all potentials are referred to. The working electrode was a gold electrode (surface 0.2 cm^2) patterned on a 9 MHz quartz crystal resonator (TEMEX, France). All solutions were freshly prepared with distilled and deionized water (MilliQ-plus, Millipore, resistivity 18.2 MΩ cm).

2.1. Film preparation

The polymerization solution was 0.25 M KNO_3 (99%, Scharlau) and 0.01 M EDOT (97%, Sigma-Aldrich) aqueous solution, pH = 7.06, and the film was generated at room temperature by applying 1.1 V during 14 s. The potential was controlled by the AUTOLAB PGSTAT 302. Before any characterization, PEDOT films were cycled between −0.8 V and 0.8 V at 50 mV s^{-1} in 0.1 M $LiClO_4$ (>95%, Sigma-Aldrich) aqueous solution until a stable current is observed. PEDOT films show a repetitive response after the first cycle in the $LiClO_4$ aqueous solution.

2.2. Spectroelectrogravimetry

PEDOT film was cycled between −0.6 V and 0.8 V at 100, 50, and 25 mV s^{-1} and between −0.8 and 0.8 V at 10 mV s^{-1} in a 0.1 M $LiClO_4$ aqueous solution (pH = 5.3) and, at room temperature. A QCM-R (RQCM, Maxtek Inc) microbalance and a Vis-NIR spectrometer (Maya 2000, Ocean optics) record gravimetric, motional resistance, and spectroscopic responses during the voltammetric cycles [28,34].

2.3. Impedance and ac-electrogravimetry

Electrochemical Impedance Spectra (EIS) and ac-electrogravimetry (or Mass Impedance Spectroscopy) were obtained in identical cell conditions. Impedance data were recorded from 65 kHz to 0.01 Hz, with 5 points per decade with 25 mV *rms* of potential perturbation amplitude. A home-made software based on the Marquardt least-squares procedure was used for the equivalent circuit fittings [57,58].

The ac-electrogravimetry was performed using a PAR 263A galvanostat-potentiostat, a SOLARTRON 1254A signal generator + frequency response analyzer and the frequency generator AGILENT 33220A. The microbalance was a lab-made oscillator built at UPR 15 CNRS Paris, France. All this equipment was controlled by home-made software. Set-up explained in recent publications [39,40,45].

3. Results and discussion

3.1. Electrogeneration of PEDOT in aqueous solution

Fig. 1 shows changes in current, mass derivative (dm/dt) and motional resistance derivative (dR_m/dt) during the electrogeneration of PEDOT films in a 0.25 M KNO_3 and 0.01 M EDOT aqueous solution expressed as time-derivative forms (dm/dt, dR_m/dt). The first step corresponds with the oxidation of monomers and the coupling of radical cation which causes the current increase until t = 1.6 s (Fig. 1A). Once the chain length of the oligomers is high enough, the polymer nuclei precipitate on the electrode surface [54] and mass increases quickly ($dm/dt > 0$ in Fig. 1A). After a short time lapse, the polymer doping caused by their oxidation also affects the mass evolution. Exchange of anions and/or solvent is needed to keep the film electroneutrality. In Fig. 1B, this process is detected by the decrease in the mass/charge ratio (Fdm/dq) (Eq. (2)) since the mass associated to the polymerization process proves larger than the mass associated with the polymer doping during the oxidation.

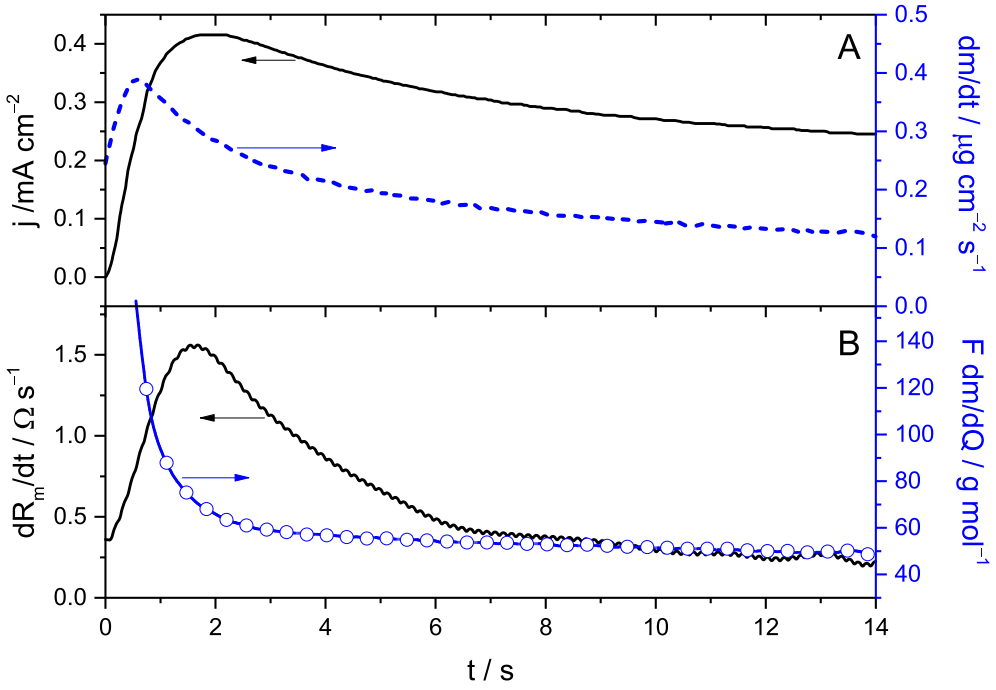

Fig. 1. PEDOT electrodeposition applying 1.1 V during 14 s in a 0.25 M KNO_3 and 0.01 M EDOT aqueous solution. (A) Current and time-derivative of mass during electrodeposition time. (B) time-derivative of R_m and Fdm/dQ function during electrodeposition time.

In those concerning viscoelastic properties, R_m keeps unchanged during the beginning of generation of the polymer nuclei, $dR_m/dt \cong 0$ in (Fig. 1B), which means that the electrode|solution interface does not change significantly. Once PEDOT chains cover partially the electrode surface, R_m starts increasing ($dR_m/dt > 0$) at 0.28 s due to the increasing friction between the electrode surface and solution. The maximum change of R_m takes place at 1.6 s when current intensity also proves maximum. This maximum of current has been reported as a maximum number of nuclei on the electrode surface [59]. Therefore, we assume that the electrode surface is fully covered by at least one layer of EDOT nuclei at this point.

After this time, previous studies have shown that the diffusion of the monomer from the solution to the electrode surface controls the polymerization rate [54,60]. Fig. 1A shows that dm/dt decreases (mass increases, but slower than before) controlled by mass transport. Fdm/dq in Fig. 1B provides more precise information about the mechanism of PEDOT polymerization in aqueous media in this growth stage. First, we assume that one electron is transferred for the formation of one radical cation of EDOT (142.18 g mol^{-1}) which is linked to the polymer chain [61] increasing the measured mass. Besides, we can consider that this new PEDOT chain is oxidized assuming another electron transfer together with the doping of one nitrate anion (62.01 g mol^{-1}) to keep the electroneutrality. Therefore, for the hypothetical overall process, the following reaction can be stated:

$$< Polymer > + EDOT + NO_3^- \rightarrow < Polymer - EDOT, NO_3^- > + 2e^- \quad (3)$$

Accordingly, $F(dm/dq)$ should reach values near $\frac{142.08+62.01}{2} \approx +102\ g{\cdot}mol^{-1}$, however, the experimental value for this function and for deposition times >7 s is about + 54 g mol^{-1} (Fig. 1B). This discrepancy can be explained by both: the anion insertion causes the opposite flux of water molecules (ξ in Eq. (2)) and also, that at these potentials there are parallel electrochemical reactions not causing deposited polymer such as water oxidation, formation of cation radicals not involving polymerization or releasing of soluble oligomers [62]. Moreover, a fast estimation of polymerization efficiency of about 50% can be obtained from the real $Fdm/dQ + 54\ g{\cdot}mol^{-1}$ values if compared with the theoretical $+102\ g{\cdot}mol^{-1}$. Anyway, R_m continues increasing during the polymerization process since $dR_m/dt > 0$ (Fig. 1B) due to the polymer growth on the gold surface, but slowly. Finally, the electrodeposition process in aqueous solution results in a blueish PEDOT film doped with NO_3^-.

3.2. Electrochemical characterization of PEDOT

3.2.1. Cyclic voltammetry

The electrochemical response of PEDOT films was first investigated by cyclic voltammetry in $LiClO_4$ aqueous solutions. The first voltammogram appears slightly different since there is the exchange between the inner NO_3^- anions and ClO_4^- anions, but after, PEDOT films show repetitive voltammograms and we can assume that all accessible NO_3^- anions inserted during the electrodeposition were substituted by ClO_4^- anions [17]. Fig. 2A shows the current response of a PEDOT film at 10 mV s^{-1}. From −0.1 V to 0.8 V, PEDOT shows the characteristic capacitive behavior with an overlapped oxidation peak at 0.21 V (peak I), which means the accumulation of positive charges along the chain. From −0.1 V to negative potentials, PEDOT shows an increasingly negative current and a clear reduction peak appears (peak II) at −0.35 V. Some authors attribute this extra current to the O_2 reduction reaction[63]. We have tested that in deaerated solutions this peak disappears (See Fig. S1, supplementary material).

As the scan rate increases, the capacitive behavior proves more evident in the whole range of potentials (Fig. 2B)[64]. Current of peak I increases linearly with scan rate (Fig. 2C) while current of peak II changes also linearly but with the square root of scan rate (Fig. 2D). This last one could mean a diffusive transport for this electrochemical process, in good agreement with the oxygen reduction reaction.

3.2.2. Spectroelectrochemical studies. Molecular information

Spectroscopic information of PEDOT films was recorded simultaneously with cyclic voltammetry. Fig. 3A shows the Vis-NIR spectra at different potentials for PEDOT films. As the potential is increasingly negative, PEDOT absorbance increases in the range 400–750 nm (light intensity or the number of counts decrease) since the film turns into a deep blue color when reaches the reduced form due to the coplanar

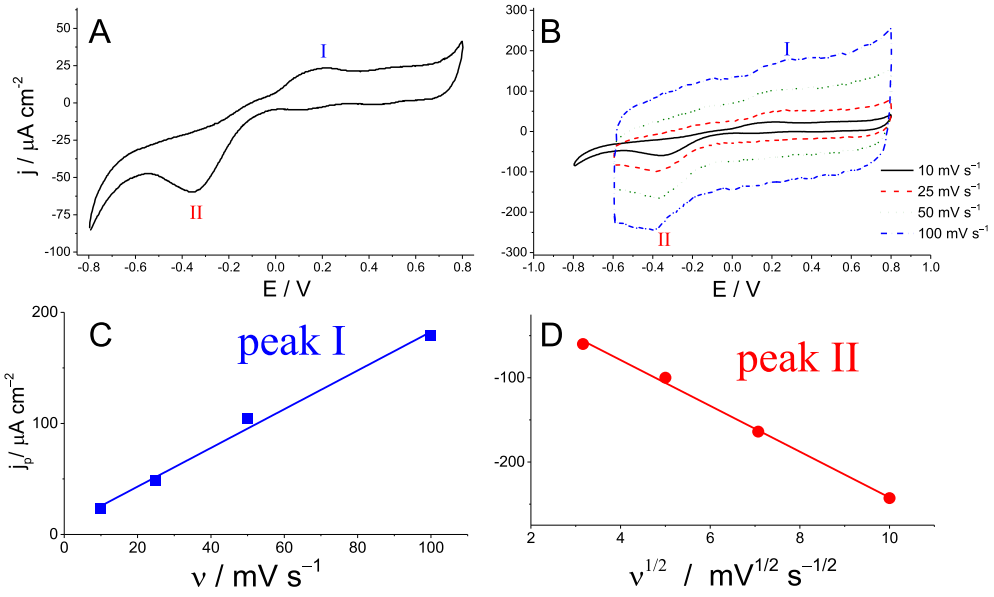

Fig. 2. (A) Voltammetry of PEDOT at 10 mV s^{-1} in 0.1 M aqueous $LiClO_4$. (B) Scan rate effect on the cyclic voltammogram of PEDOT. (C) Peak I current against *scan rate* (D) Peak II current against the square root of scan rate.

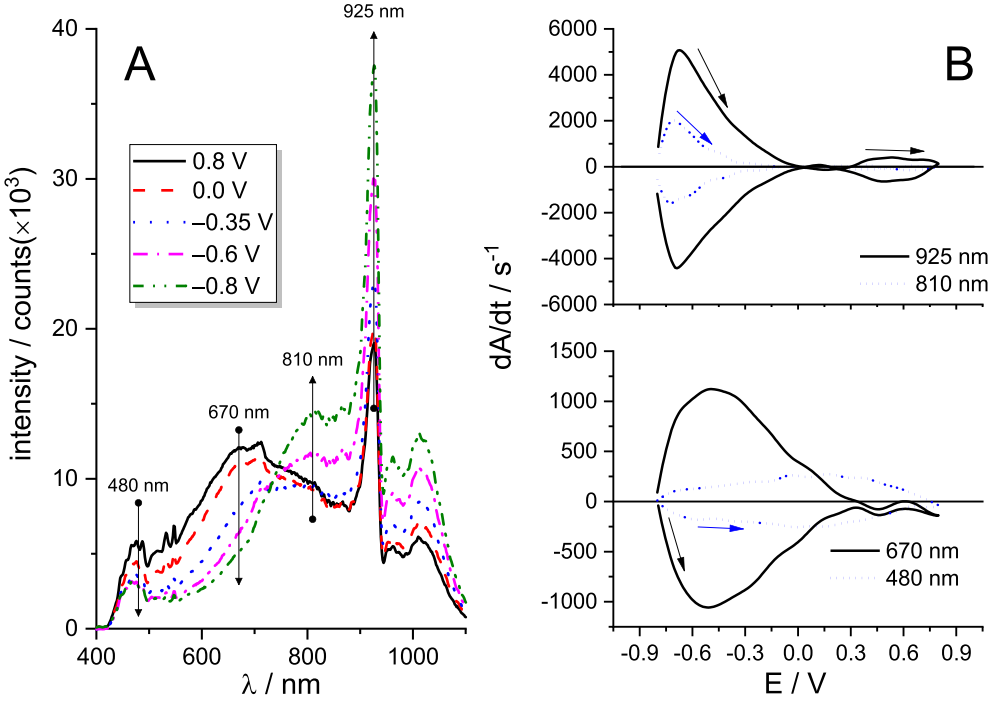

Fig. 3. Spectroelectrochemical characterization of PEDOT films at a scan rate of 100 mV s^{-1} in a 0.1 M $LiClO_4$ aqueous solution. (A) The vis-NIR spectrum between 400 nm and 1100 nm at some potential. (B) dA^{λ}/dt against the potential between −0.8 V and 0.8 V at the characteristics wavelengths.

aromatic heterocycles of the backbone and two electron-donating oxygen atoms coupled to the thiophene ring, which contribute to the π-π* transitions [65,66]. This interval of wavelengths is usually associated with the $\pi \rightarrow \pi^*$ transition of the thiophene rings [67,68]. On the other hand, absorbance in the wavelengths range of 750–1100 nm increases as the PEDOT is oxidized, mostly at potentials from −0.8 V to −0.2 V. The oxidation of neutral PEDOT involves the formation of polaron that together with the doping increases the metallic type conduction of film [65,69,70].

These spectra were presented as number of counts at each wavelength since it is not possible a zero absorbance reference spectrum at all the studied wavelengths, and therefore it is not possible an absolute value of absorbance. However, the time derivative absorbance against potential curves are possible. To further characterize the mechanism of electrochemical processes in PEDOT films it is preferred the time derivative of absorbance at a wavelength λ (dA^{λ}/dt). This function provides specific information about the electrochemical processes of PEDOT discarding capacitive and secondary reaction currents which do not cause absorbance changes and also because dA^{λ}/dt does not require knowing the blank absorbance value[71]. dA^{λ}/dt is easily obtained from the number of counts (n_c^{λ}) of a digital spectrometer at

the wavelength λ by considering that light intensity at this wavelength (I^{λ}) is proportional to this number of counts:

$$I^{\lambda} \propto n_c^{\lambda};\quad I^{\lambda} = Kn_c^{\lambda} \tag{4}$$

$$A^{\lambda} = -\log\left(\frac{I^{\lambda}}{I_0^{\lambda}}\right) = \log\left(I_0^{\lambda}\right) - \log\left(I^{\lambda}\right) \tag{5}$$

$$\frac{dA^{\lambda}}{dt} = -\frac{dlog\left(Kn_c^{\lambda}\right)}{dt} = -\frac{dlog\left(n_c^{\lambda}\right)}{dt} \tag{6}$$

where I_0^{λ} represents the light intensity for the blank sample at a wavelength λ, and K an arbitrary constant relating color intensity and the number of counts.

It should be noted that dA^{λ}/dt proves proportional to the number of active centers that change during the electrochemical redox process of the polymer, dn_{ac}/dt, as it occurs with the current associated with this faradaic process.

$$A^{\lambda} = \varepsilon^{\lambda} \cdot A \cdot n_{ac} \tag{7}$$

$$\frac{dA^{\lambda}}{dt} = \varepsilon^{\lambda}\frac{dn_{ac}}{dt} \tag{8}$$

where ε^{λ} represents an apparent electrochromic efficiency for the change of concentration of active centers at the λ wavelength[71,72].

In Fig. 3B, dA^{λ}/dt curves at four selected wavelengths (480, 670, 810 and 925 nm) are plotted. If compared with current curves, the first observation is the zero baseline at all selected wavelengths that indicates that a part of the measured current should be caused by a parallel electrochemical process causing no color change: the hydrogen production at negative potentials, the oxygen formation at more positive potentials, and also, the molecular O_2 reduction since the solution was not deaereated. Anyway, not all the electrochemical processes cause color changes at all the studied wavelengths.

The formation of polaron structures from neutral PEDOT is revealed by reversible dA^{810}/dt peaks around -0.7 V [65]. At E $>$ -0.2 V there is no significative change of absorbance at $\lambda = 810$ nm, therefore, no more polarons are accumulated beyond this potential. By further oxidation of PEDOT films, bipolaron structures are rapidly accumulated around -0.6 V (dA^{925}/dt peaks)[65]. Nearby, the switching between deep blue and light blue PEDOT could be associated with changes at 670 nm (visible wavelength) and peaks of dA^{670}/dt appear also slightly displaced towards positive potentials than dA^{925}/dt peaks[66]. The complete color conversion is reached at 0.4 V where $dA^{670}/dt = 0$. It should be noted that there is no wavelength associated with the peak II in the voltammogram. As a result, the current associated with the formation of polaron and bipolaron structures at these potentials could be masked by the high current of another overlapped electrochemical processes.

Around potentials near 0.0 V, where peak I takes place, dA^{480}/dt reaches negative values during the oxidation (Fig. 3B). This wavelength could be related to the disappearance of neutral PEDOT units by oxidation since the absorbance decreases as PEDOT is oxidized and vice versa. Absorbance at 480 nm changes during all the PEDOT charge/discharge process. The dA^{480}/dt curve is very similar to that of a supercapacitor typical current and we can assume that changes at this wavelength are associated with the capacitive behavior of the polymer. Around 0.4 V, dA^{925}/dt shows a second peak couple which could be associated with a new formation of bi-polarons in the film [65]. Finally, no significant absorbance changes are observed at $E > 0.7$ V. Hence, the extra current observed in the voltammogram should be attributed to other electrochemical reactions of the media, such as the water oxidation.

3.2.3. Electrogravimetry study in the dc-regime

Mass changes accompanying redox processes in conducting polymers are mostly caused by the exchange of counterions to keep the film electroneutrality. From -0.8 V to -0.2 V the charge of neutral PEDOT starts with a decrease in mass (measured with an EQCM) indicating that cations leave the film (Fig. 4A). However, the overall current reaches negative values indicating that another reduction reaction is mainly taking place. At potentials of peak II (-0.38 V) mass changes are very small and at larger potentials, the charge of PEDOT involves an increase in mass due to the insertion of perchlorate anions to balance the positive charges formed [18,20].

In Fig. 4B and at potentials around peak I, Fdm/dQ (Eq. (2)) reaches values between + 32 and + 54 $g{\cdot}mol^{-1}$, far from the expected perchlorate molar mass (99.5 $g{\cdot}mol^{-1}$). We consider several possible causes for this difference: the anion exclusion effect [18,73], a partial opposite flux of cations, and the existence of an extra current due to electrochemical redox processes of the outer solution. The latter is corroborated by the sudden current increase near + 0.8 V involving that Fdm/dq falls to 0.

During PEDOT discharge from -0.2 V to -0.8 V, Fdm/dQ moves from $+4.2$ g mol^{-1} to -9.7 g mol^{-1} confirming the cation participation. This is similar to results presented by other authors [62]. This low value compared with the expected hydrated Li^{+} cation mass could also be explained by the partial participation of anions and/or other faradaic processes without mass contribution. For this purpose, ac-electrogravimetry allows separating the contribution of different species by their relative time constants[37,38].

3.2.4. Electrochemical impedance spectroscopy and ac-electrogravimetry

The above results allow us to state that more than one process should be considered for a good interpretation. Hyphenated techniques in the dc-regime allow to identify the partial participation of each one of the processes in the overall response, but it proves not easy to separate according to their relative rates. For that purpose, it is preferably the use of hyphenated techniques in the ac-regime, or in other words, the coupling of electrochemical impedance spectroscopy (EIS) and ac-electrogravimetry[37,39,74]. Fig. 5 shows complex plane capacitance plots of PEDOT films at different potentials. Capacitance plots are useful for describing impedance spectra for conducting polymers and is obtained from impedance as:

$$C(\omega) = \frac{\Delta q}{\Delta E}(\omega) = \frac{1}{j\omega}\left(\frac{\Delta E}{\Delta i}(\omega)\right)^{-1} \tag{9}$$

where j is the imaginary number and ω is the angular frequency.

We use a model to analyze these impedance spectra based on the hypothesis of two electrochemical processes taking place. Therefore, our equivalent circuit has two branches in parallel describing both faradaic processes (Fig. 5). The RC branch is associated with a fast charge/discharge process in the electroactive polymer[25,39,58], the R_{ct} element represents the fast charge transfer resistance for this process and the capacitance C is a mesure of the amount of electrical charge in the supercapacitor polymer. The other branch is associated with the low frequencies response. The Warburg element represents the impedance associated with a faradaic reaction controlled by the diffusion of electroactive species towards the electrode surface and the resistance a charge transfer resistance for this process. In our case, this reaction can be the O_2 reduction, the hydrogen evolution reaction at the more negative potentials or the water oxidation at the more positive potentials and is responsible for the low frequencies line in the capacitance plot of Fig. 5. The resistance R_2 represents the charge transfer resistance for this process.

Experimental data were fitted to this model and Table 1 collects parameters obtained. In all the potential range, the double layer capacitance (C_{dl}) and the uncompensated resistance (R_u) do not change sig-

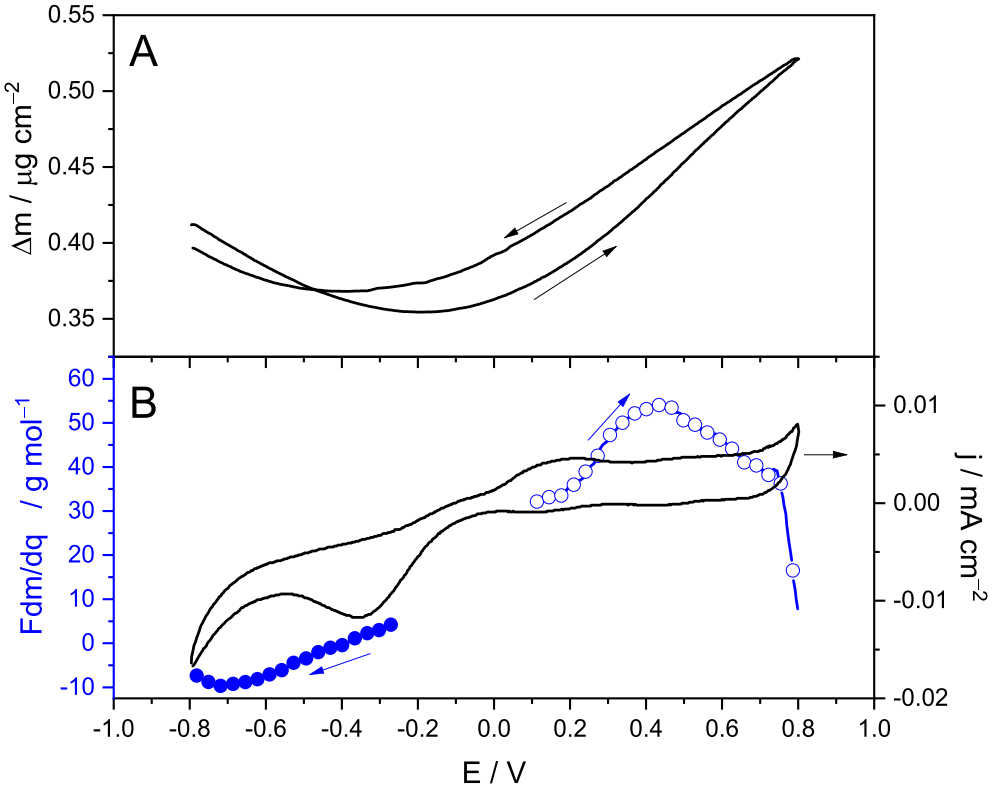

Fig. 4. Electrogravimetry of PEDOT film in 0.1 M $LiClO_4$ aqueous solution at 10 mV s^{-1}. (A) mass changes and (B) *Fdm/dq* during charge of PEDOT (open circles) and during discharge of PEDOT (closed circles) and cyclic current response.

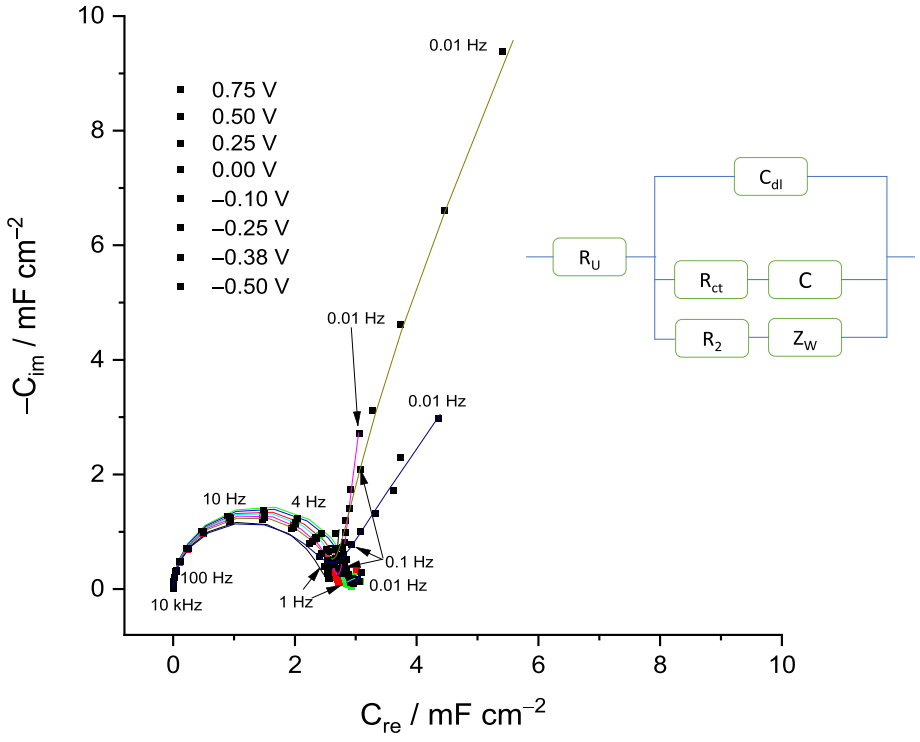

Fig. 5. Complex plane impedance diagrams for PEDOT at different potentials. The dotted representation corresponds to the experimental values and the continuous line to the fitting to the equivalent circuit. Ru is the uncompensated resistance, Cdl is the double layer capacitance, R, C and Z_W are the charge transfer resistance, capacitance and Warburg impedance for the processes 1 and 2.

Table 1
Values of parameters obtained from the fitting of experimental EIS data to the equivalent circuit model in Fig. 5. Impedance associated to the Warburg element is given by $Z_W = \frac{(1-j)}{\sqrt{\omega}}\sigma$

E V	Ru Ω	C *mF*	R_2 *kΩ*	σ $\Omega s^{-0.5}$	Cdl *μF*
−0.60	32	0.63	17		4.5
−0.50	32	0.65	5.6	2400	4.5
−0.38	32	0.68	4.1	485	4.5
−0.25	32	0.68	20	730	4.5
−0.10	32	0.72			4.5
0.00	32	0.70			4.5
0.25	32	0.69			4.5
0.50	32	0.66			4.5
0.75	32	0.65	60		4.5

nificantly, and we can fix these values to 4.5 μF and to 32 Ω, respectively, both estimated from high-frequency impedance.

The fastest process shows a very low charge transfer resistance (R_{ct}) that keeps constant around 1 Ω, a value smaller than the uncertainty of this parameter from the fitting, that could explain the fast charge-discharge properties of this polymer. Capacitance (C) reaches values between 0.63 mF and 0.72 mF, the larger ones at potentials between −0.38 and 0.25 V. These huge values are in good agreement with the large capacitive currents observed in the cyclic voltammetry. As a result, a very similar capacitance loop appears at all the studied potentials in Fig. 5 [18,75-77].

The slowest process is only possible if there is a secondary overlapped reaction. In the potential range between −0.5 and −0.2 V, this reaction is the O_2 reduction and Warburg like impedance is shown characterized by a 45° line. At the more positive potentials, this secondary reaction could be the water oxidation but no Warburg impedance can be measured since there is no transport control, in contrast a 90° phase in the capacitance plot is observed, equivalent to 0° in the impedance plot characteristic for a resistive behavior (R_2). For the more negative potentials (−0.6 V), the hydrogen evolution reaction takes place, but no mass control is observed in Fig. 5, only a resistance.

Even though EIS gives rich information about the rate of the different processes, there is no information about the role of cations, anions, and solvent during these processes. For this purpose, ac-electrogravimetry has been revealed as a powerful tool allowing to discern the role of different species during electrochemical processes depending on the loop shapes and where these loops appear on the ac-electrogravimetry complex plane plot [18,37-39,41]. Comparing Fig. 5 and Fig. 6, one can see in Fig. 6 only one semicircle at all the studied potentials without any trace of a second process at the lowest frequencies for the ac-electrogravimetry experiment, however this semicircle changes its size and the quadrant on the complex plane. Between −0.1 V and 0.8 V, semicircles on the first quadrant indicate the main participation of anions in the charge/discharge process of PEDOT [39,45,74]. On the contrary, semicircles on the third quadrant at potentials below −0.2 V indicate the main participation of cations [39,45,74]. Noticeably, there is no transition between quadrants (no loop on the second or on the fourth quadrant) expected for two ions transitions with different time constants. Therefore, cation and anion exchanges

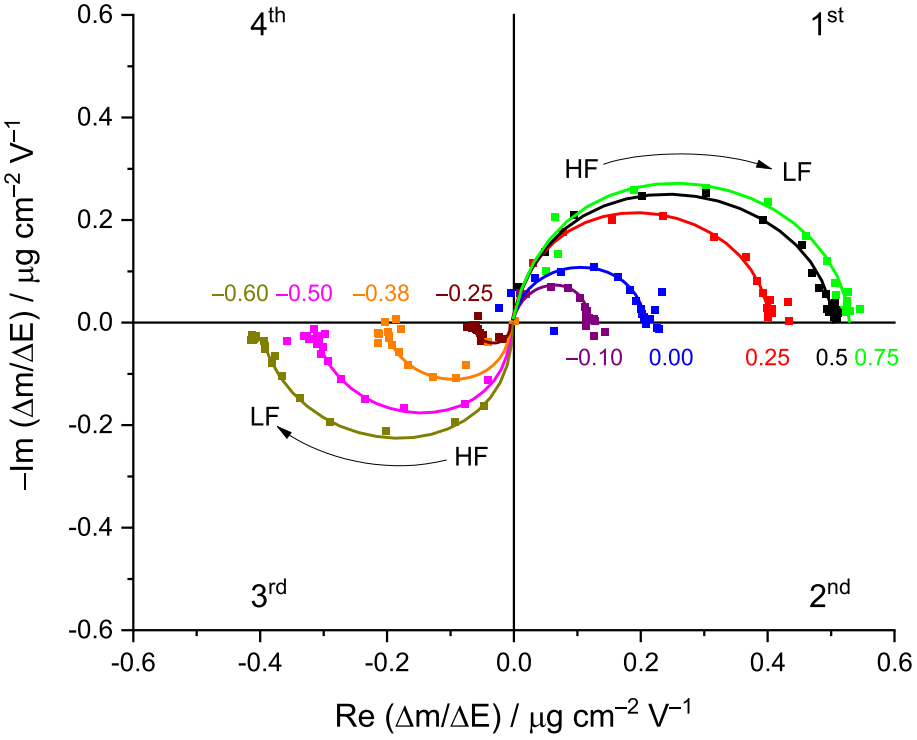

Fig. 6. ac-electrogravimetry spectra obtained for PEDOT in 0.1 M $LiClO_4$ aqueous solutions at different potentials. Arrows indicate the transition between high frequencies (HF) and low frequencies (LF). Potentials are marked on the Real Part axis.

are caused by the same electrochemical process in the PEDOT film with an identical time constant. Alternatively, the electron transport through the polymer could be the rate-determining step for this electrochemical process. From our results, it is not possible to discern between both possibilities.

Another important information is given by the size of the ac-electrogravimetry semicircle, the largest the semicircle the largest the mass change. In other polymers, ac-electrogravimetry data show the largest semicircle at those potentials corresponding to the maximum of peak currents during the voltammogram [23,37,39]. Here, maximum cation semicircle (3rd quadrant) is obtained for the most negative potential and the maximum anion one (1st quadrant) for the most positive potential.

In order to deep into the information obtained by EIS and ac-electrogravimetry, the mixed transfer function $F\Delta m/\Delta q(\omega)$ is analyzed (Fig. 7). This function is obtained from the ac-electrogravimetry transfer function, $\frac{\Delta m}{\Delta E}(\omega)$, and the capacitance one (Eq. (9)) from Eq. (1)

Their physical interpretation is similar to that of Eq. (2) allowing to discern the relative participation of different species in the overall process. If two different ions exchange and these processes are overlapped with different time constants, this transfer function provides both, a real part and the imaginary part of a complex number. However, our experimental results (Fig. 7) show that the imaginary part of this transfer function takes values near 0 and the real one keeps constant in a wide range of frequencies from 10 to 0.1 Hz for all investigated potentials. Therefore, one can conclude that only one process is responsible for the mass changes [40,41].

In the range of potentials between −0.1 V and 0.75 V positive values of $F\Delta m/\Delta q(\omega)$ mean a large participation of anions as counterions. These values increase from 20 g·mol^{-1} at −0.1 V up to 80 g·mol^{-1} at + 0.75 V. For a pure perchlorate exchange a value of 99.5 g·mol^{-1} should be expected. Since in this range of potentials no other chemical reaction is coupled, the smaller $F\Delta m/\Delta q(\omega)$ values should be attributed to the exchange of water molecules in the opposite sense by the exclusion effect and/or to the exchange of hydrated Li^+ cations. In any case, there is only one capacitive loop in the capacitance complex plot indicating that the exchange of anions, cations and water takes place simultaneously.

At potentials from −0.25 V to −0.60 V and in the range of frequencies from 0.1 Hz to 10 Hz, this function reaches values going from −5 g mol^{-1} to −65 g·mol^{-1} indicating that charge balance mainly takes place by the exchange of cations, being the largest ones in absolute value at the most negative potential, about $-65\ g{\cdot}mol^{-1}$, larger enough than Li^+ mass. That means at least 3 water molecules accompanying Li^+ cations. At frequencies smaller than 0.1 Hz, $|F\Delta m/\Delta q(\omega)|$ quickly decreases reaching values near 0 in the case of −0.38 V (peak II) for the smallest frequencies in good agreement with a secondary electrochemical reaction coupled: the catalytic O_2 reduction involving an electric charge transfer but no mass change [63]. In the impedance spectra of Fig. 5, we can see a low frequencies line at these potentials that should correspond to a process not involving mass changes since this line is not observed in ac-electrogravimetry in Fig. 6.

From several assumptions based on these results we can estimate the relative participation of cations and anions at each potential. First, we assume that both, cations and anions, can participate as counterions. Second, we consider that the entrance of anions is accompanied by the exit of some water molecules by the exclusion effect, in our case we suppose one H_2O by each ClO_4^- anion since the largest value for the $F\Delta m/\Delta q$ is about +80 g mol^{-1}. Finally, for the lithium participation we assume that × water molecules accompany each lithium cation, that means a mass change of $-(7 + 18x)\ g{\cdot}mol^{-1}$. Therefore, we can obtain an expression for the $\Delta m/\Delta q(\omega)$:

$$F\left(\frac{\Delta m}{\Delta q}\right)(\omega) = a \cdot A \cdot \left(-(7+18x)\ g \cdot mol^{-1}\right) + (1-a) \cdot A \cdot \left(81\ g \cdot mol^{-1}\right) \tag{10}$$

where a represents the relative participation of lithium cations in the charge balance and $(1-\ a)$ the relative participation of perchlorate anions.

Fig. 8 shows the estimated dependence on the applied potential of this relative participation for both ions and for different values of x. For the anion participation, our assumption seems to be right since their relative participation does not vary too much from potentials +0.6 to +0.75 V. For the cation one, it seems than >3 water

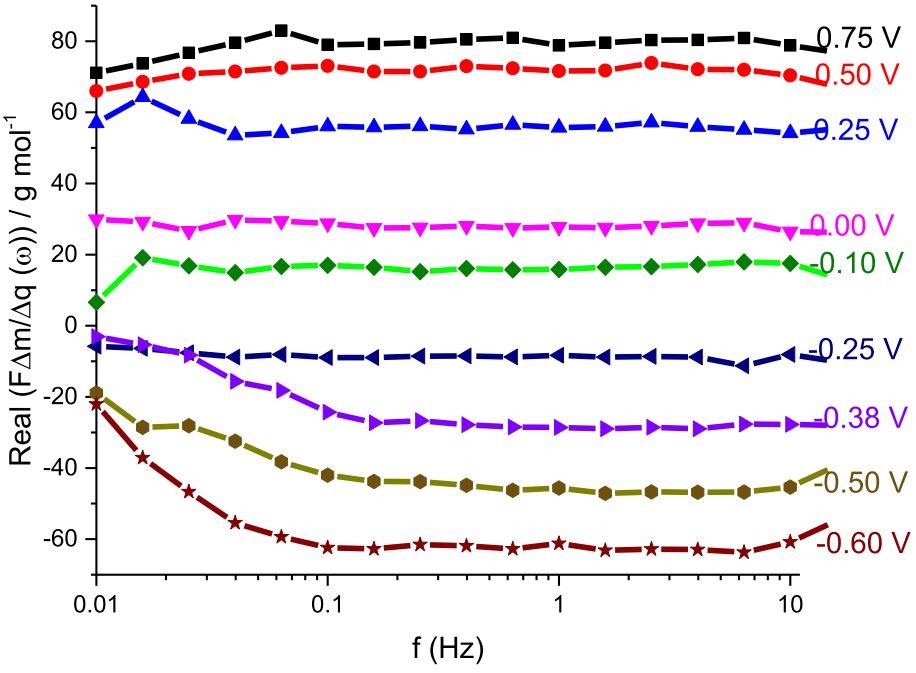

Fig. 7. Representation of Re (F·Δm/ΔQ) at each frequency for different potentials of interest.

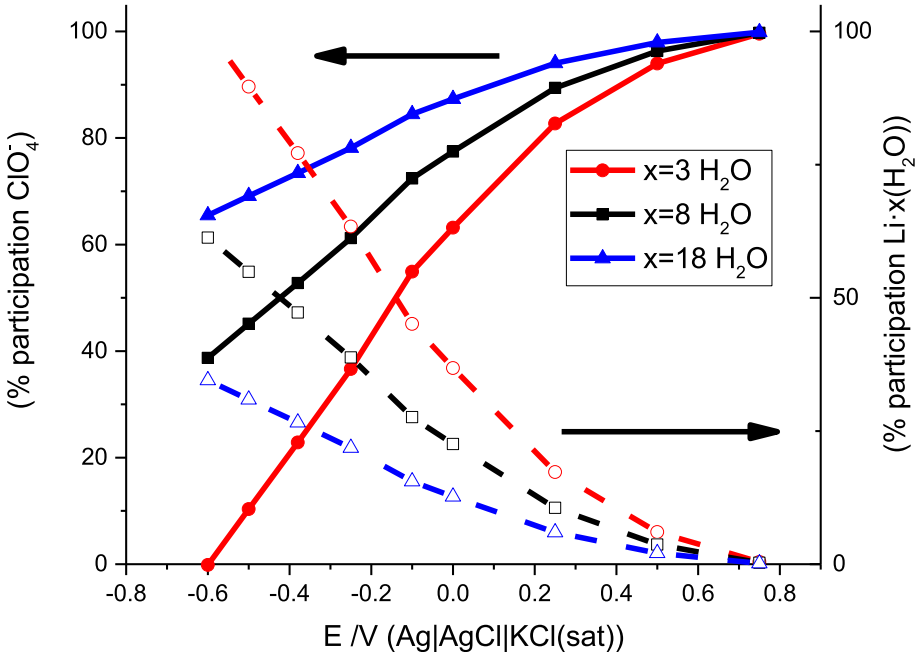

Fig. 8. Relative participation of cations (open symbols) and anions (filled symbols) during the charge balance process assuming that Li^+ enters solvated by $\times$ H_2O molecules and that each ClO_4^- excludes 1 H_2O molecule.

molecules can accompany the Li^+ cation. Therefore, at more negative potentials, the semicircle corresponding to the ac-electrogravimetry should be greater than this one obtained at $E = -0.6V$. However, the stability of the film should be compromised at these potentials. In any case, the participation of cations at potentials $E > 0.2V$ seems very small, while at potentials $E < -0.4$ V could be more important.

Then, we simulated different possibilities for $x = 3, 8$ *or* 18 water molecules. Looking at Fig. 8 values of $x = 18$ imply that at potentials $E < -0.6V$ the relative participation of anions should be negative and the cations participation >100%. We can discard this possibility and, therefore, a smaller number of water molecules accompanying Li^+ cations should be considered. An intermediate value between 3 and 18 ($x = 8$) seems the most acceptable one.

3.2.5. Viscoelasticity

The hydration of PEDOT influenced by the anion exclusion, Li hydration or conformational rearrangement can change the viscoelastic properties of the film, which can be monitored by changes of the motional resistance (R_m). Between -0.8 V and -0.2 V, the insertion of Li^+ cations hardly hydrated, as $F\Delta m/\Delta q$ suggests, makes this film softener increasing the R_m values (Fig. 9). However, at potentials around peak I, R_m keeps almost constant. The accumulation of a higher

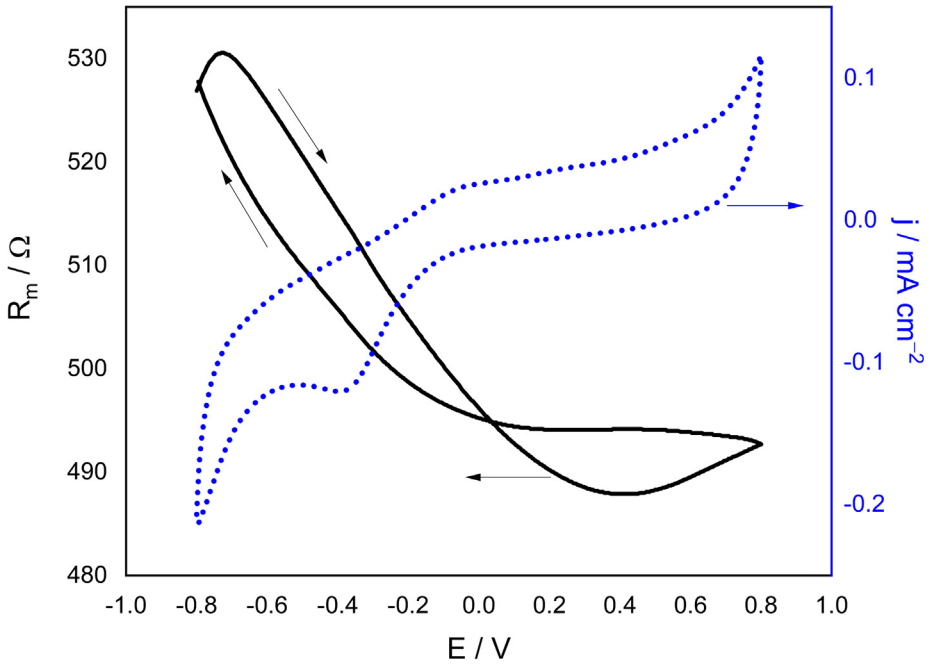

Fig. 9. Variation of the electromechanical resistance, R_m with the potential at a scan rate of 50 mV·s^{-1} in 0.1 M $LiClO_4$.

population of charge-balancing counterions ("dopants") generating electrostatic interactions between polymer chains and ions together with the dry of PEDOT by the exclusion effect during the PEDOT charge cause the film stiffness [28,78,79] and then, the decrease of the R_m value. Therefore, as Fig. 8 and Fig. 9 suggest, an important exchange of water molecules accompanied by the Li^+ cation occurs at the more negative potentials.

4. Conclusions

The yield of electrodeposited mass was about 50% of the expected mass, including the anion doping of the generated polymer.

The electrochemical behavior of PEDOT films in $LiClO_4$ aqueous solutions should be described as the overlap of at least two well-separated electrochemical processes. On the one hand, there is the electrochemical charge and discharge reactions of PEDOT, identified as the fast process that needs the exchange of counterions. The insertion/expulsion of Li^+ is accompanied by several water molecules and the anions exchange involves an opposite flux of water due to the anion exclusion effect. Both, cation and anion, exchange processes take place with the same time constant and their relative participation can be estimated from $F\Delta m/\Delta q(\omega)$ function and depends on the applied potential. At more negative potentials, the larger cation participation, and the opposite for the more positive potentials. This is also confirmed by the change of R_m on the applied potentials, reaching maximum values in the more negative potentials where the film proves more hydrated by the insertion of hydrated Li^+ cations.

The second electrochemical process, the slow one, proves maximum at the potential where a voltammetric peak appears (E = -0.38 V). This process can be attributed to the O_2 reduction and does not cause any mass change, nor color changes of the polymer. The peak current dependence on the square root of the scan rate indicates a mass transport control in good agreement with this hypothesis, also a Warburg behavior of the low-frequencies impedance spectra.

All these results evidence the rich information obtained from hyphenated techniques in the dc and ac regimes, mainly if crossed functions are obtained from experimental results of different techniques as it could be the Fdm/dq in the dc-regime (EQCM + CV) or the $F\Delta m/\Delta q(\omega)$ in the ac-regime (EIS + MIS). This experimental strategy has proved useful for the design and characterization of supercapacitors based on the simultaneous accumulation of fast ionic species during electrochemical redox processes of the polymeric material.

CRediT authorship contribution statement

E. Guillén: Conceptualization, Methodology, Writing-review & editing. **J. Agrisuelas:** Conceptualization, Methodology, Writing - review & editing, Supervision. **J.J. García-Jareño:** Conceptualization, Methodology, Writing-review & editing, Supervision. **F. Vicente:** Supervision, Conceptualization, Methodology, Writing - review & editing.

Declaration of Competing Interest

The authors declare that they have no known competing financial interests or personal relationships that could have appeared to influence the work reported in this paper.

Acknowledgments

This work was supported by MINECO-FEDER project CTQ2015-71794-R and CTQ2017-90659-REDT (MEIC/AEI, Spain). The invitation by the E3TECH Spanish Network of Excellence (CTQ2017-90659-REDT (MEIC/AEI)) is kindly acknowledged.

Appendix A. Supplementary data

Supplementary data to this article can be found online at https://doi.org/10.1016/j.jelechem.2021.115580.

References

[1] L. Groenendaal, F. Jonas, D. Freitag, H. Pielartzik, J.R. Reynolds, Poly(3,4-ethylenedioxythiophene) and its derivatives: past, present, and future, Advanced Materials. 12 (2000) 481–494, https://doi.org/10.1002/(SICI)1521-4095(200004)12:7<481::AID-ADMA481>3.0.CO;2-C.
[2] S. Kirchmeyer, K. Reuter, Scientific importance, properties and growing applications of poly(3,4-ethylenedioxythiophene), J. Mater. Chem. 15 (2005) 2077–2088, https://doi.org/10.1039/B417803N.
[3] Y. Wang, Y.u. Ding, X. Guo, G. Yu, Conductive polymers for stretchable supercapacitors, Nano Res. 12 (9) (2019) 1978–1987, https://doi.org/10.1007/s12274-019-2296-9.
[4] A. Muzaffar, M.B. Ahamed, K. Deshmukh, J. Thirumalai, A review on recent advances in hybrid supercapacitors: Design, fabrication and applications, Renewable and Sustainable Energy Reviews. 101 (2019) 123–145, https://doi.org/10.1016/j.rser.2018.10.026.
[5] Z.-Q. Feng, J. Wu, W. Cho, M.K. Leach, E.W. Franz, Y.I. Naim, Z.-Z. Gu, J.M. Corey, D.C. Martin, Highly aligned poly(3,4-ethylene dioxythiophene) (PEDOT) nano- and microscale fibers and tubes, Polymer. 54 (2) (2013) 702–708, https://doi.org/10.1016/j.polymer.2012.10.057.
[6] M. Vázquez, J. Bobacka, M. Luostarinen, K. Rissanen, A. Lewenstam, A. Ivaska, Potentiometric sensors based on poly(3,4-ethylenedioxythiophene) (PEDOT) doped with sulfonated calix[4]arene and calix[4]resorcarenes, Journal of Solid State Electrochemistry. 9 (5) (2005) 312–319, https://doi.org/10.1007/s10008-004-0597-7.
[7] F. Jonas, J.T. Morrison, 3,4-polyethylenedioxythiophene (PEDT): Conductive coatings technical applications and properties, Synthetic Metals. 85 (1-3) (1997) 1397–1398, https://doi.org/10.1016/S0379-6779(97)80290-1.
[8] T.M. Brown, J.S. Kim, R.H. Friend, F. Cacialli, R. Daik, W.J. Feast, Built-in field electroabsorption spectroscopy of polymer light-emitting diodes incorporating a doped poly(3,4-ethylene dioxythiophene) hole injection layer, Appl. Phys. Lett. 75 (12) (1999) 1679–1681, https://doi.org/10.1063/1.124789.
[9] J.-H. Huang, D. Kekuda, C.-W. Chu, K.-C. Ho, Electrochemical characterization of the solvent-enhanced conductivity of poly(3,4-ethylenedioxythiophene) and its application in polymer solar cells, Journal of Materials Chemistry. 19 (2009) 3704–3712, https://doi.org/10.1039/b822729b.
[10] G.A. Snook, P. Kao, A.S. Best, Conducting-polymer-based supercapacitor devices and electrodes, Journal of Power Sources. 196 (1) (2011) 1–12, https://doi.org/10.1016/j.jpowsour.2010.06.084.
[11] M.S. Cho, H.J. Seo, J.D. Nam, H.R. Choi, J.C. Koo, K.G. Song, Y. Lee, A solid state actuator based on the PEDOT/NBR system, Sensors and Actuators, B: Chemical. 119 (2) (2006) 621–624, https://doi.org/10.1016/j.snb.2006.01.021.
[12] D.-H. Kim, S.M. Richardson-Burns, J.L. Hendricks, C. Sequera, D.C. Martin, Effect of immobilized nerve growth factor on conductive polymers: Electrical properties and cellular response, Advanced Functional Materials. 17 (1) (2007) 79–86, https://doi.org/10.1002/(ISSN)1616-302810.1002/adfm.v17:110.1002/adfm.200500594.
[13] A.R. Hillman, S.J. Daisley, S. Bruckenstein, Kinetics and mechanism of the electrochemical p-doping of PEDOT, Electrochemistry Communications. 9 (6) (2007) 1316–1322, https://doi.org/10.1016/j.elecom.2007.01.009.
[14] A.R. Hillman, S.J. Daisley, S. Bruckenstein, Solvent effects on the electrochemical p-doping of PEDOT, Physical Chemistry Chemical Physics. 9 (2007) 2379–2388, https://doi.org/10.1039/B618786B.
[15] A. Bund, S. Neudeck, Effect of the Solvent and the Anion on the Doping/Dedoping Behavior of Poly(3,4-ethylenedioxythiophene) Films Studied with the Electrochemical Quartz Microbalance, J. Phys. Chem. B. 108 (46) (2004) 17845–17850, https://doi.org/10.1021/jp0469721.
[16] W. Plieth, A. Bund, U. Rammelt, S. Neudeck, LeMinh Duc, The role of ion and solvent transport during the redox process of conducting polymers, Electrochimica Acta. 51 (11) (2006) 2366–2372, https://doi.org/10.1016/j.electacta.2005.03.087.
[17] T. Le, D. Aradilla, G. Bidan, F. Billon, C. Debiemme-Chouvy, H. Perrot, O. Sel, Charge Storage Properties of Nanostructured Poly (3,4-ethylenedioxythiophene) Electrodes Revealed by Advanced Electrogravimetry, Nanomaterials. 9 (2019) 962, https://doi.org/10.3390/nano9070962.
[18] J. Agrisuelas, C. Gabrielli, J.J. García-Jareño, H. Perrot, O. Sel, F. Vicente, Electrochemically induced free solvent transfer in thin poly(3,4-ethylenedioxythiophene) films, Electrochimica Acta. 164 (2015) 21–30, https://doi.org/10.1016/j.electacta.2015.02.133.
[19] J. Meng, X. Li, M. Qin, Y. Pei, S. Yang, Y. Lan, R. Wang, G. Chen, Effects of pore size of reverse opal structured PEDOT films on their electrochromic performances, Organic Electronics. 50 (2017) 16–24, https://doi.org/10.1016/j.orgel.2017.07.018.
[20] T.F. Otero, J.G. Martinez, Artificial Muscles: A Tool To Quantify Exchanged Solvent during Biomimetic Reactions, Chem. Mater. 24 (21) (2012) 4093–4099, https://doi.org/10.1021/cm302847r.
[21] M.J. Brown, A. Robert Hillman, S.J. Martin, R.W. Cernosek, H.L. Bandey, Manipulation of electroactive polymer film viscoelasticity: the roles of applied

potential and frequency, Journal of Materials Chemistry. 10 (2000) 115–126, https://doi.org/10.1039/A903820E.
[22] A. Bund, R. Peipmann, Application of PEDOT layers for the electrogravimetric detection of sulphate and phosphate in aqueous media, Electrochimica Acta. 53 (11) (2008) 3772–3778, https://doi.org/10.1016/j.electacta.2007.10.028.
[23] J. Agrisuelas, C. Gabrielli, J.J. García-Jareño, H. Perrot, F. Vicente, Effects of anion size on the electrochemical behavior of H2SO4-structured poly(o-toluidine) films, An ac-electrogravimetry study in acid solutions, Electrochimica Acta. 132 (2014) 561–573, https://doi.org/10.1016/j.electacta.2014.04.047.
[24] A.R. Hillman, M.J. Swann, S. Bruckenstein, General-approach to the interpretation of electrochemical quartz crystal microbalance data.1. Cyclic voltammetry – kinetic subtleties in the electrochemical doping of polybithiophene films, Journal of Physical Chemistry. 95 (1991) 3271–3277, https://doi.org/10.1021/j100161a056.
[25] T. Amemiya, K. Hashimoto, A. Fujishima, Investigation of dynamics of faradaic processes in polypyrrole films by electrochemical impedance and color admittance spectroscopies, Denki Kagaku. 60 (12) (1992) 1075–1081, https://doi.org/10.5796/electrochemistry.60.1075.
[26] D. Giménez-Romero, J.J. Garcı´a-Jareño, F. Vicente, EQCM and EIS studies of Znaq2 + + 2e − ⇄Zn0 electrochemical reaction in moderated acid medium, Journal of Electroanalytical Chemistry. 558 (2003) 25–33, https://doi.org/10.1016/S0022-0728(03)00373-5.
[27] J. Agrisuelas, C. Gabrielli, J.J. Garcı´a-Jareño, D. Gime´nez-Romero, J. Gregori, H. Perrot, F. Vicente, Usefulness of F(dm/dQ) function for elucidating the ions role in PB films, J. Electrochem. Soc. 154 (6) (2007) F134, https://doi.org/10.1149/1.2728038.
[28] J. Agrisuelas, C. Gabrielli, J.J. García-Jareño, H. Perrot, O. Sel, F. Vicente, Viscoelastic potential-induced changes in acoustically thin films explored by quartz crystal microbalance with motional resistance monitoring, Electrochimica Acta. 176 (2015) 1454–1463, https://doi.org/10.1016/j.electacta.2015.07.131.
[29] J.J. García-Jareño, C. Gabrielli, H. Perrot, Validation of the mass response of a quartz crystal microbalance coated with Prussian Blue film for ac electrogravimetry, Electrochemistry Communications. 2 (3) (2000) 195–200, https://doi.org/10.1016/S1388-2481(99)00168-X.
[30] H. Muramatsu, E. Tamiya, I. Karube, Computation of equivalent circuit parameters of quartz crystals in contact with liquids and study of liquid properties, Anal. Chem. 60 (19) (1988) 2142–2146, https://doi.org/10.1021/ac00170a032.
[31] S.J. Martin, V.E. Granstaff, G.C. Frye, Characterization of a quartz crystal microbalance with simultaneous mass and liquid loading, Anal. Chem. 63 (20) (1991) 2272–2281, https://doi.org/10.1021/ac00020a015.
[32] W.W. Lee, H.S. White, M.D. Ward, Depletion layer effects on the response of the electrochemical quartz crystal microbalance, Anal. Chem. 65 (22) (1993) 3232–3237, https://doi.org/10.1021/ac00070a011.
[33] Q. Xie, J. Wang, A. Zhou, Y. Zhang, H. Liu, Z. Xu, Y.u. Yuan, M. Deng, S. Yao, A Study of Depletion Layer Effects on Equivalent Circuit Parameters Using an Electrochemical Quartz Crystal Impedance System, Anal. Chem. 71 (20) (1999) 4649–4656, https://doi.org/10.1021/ac981390z.
[34] D. Gimenez-Romero, J. Agrisuelas, J.J. Garcia-Jareno, J. Gregori, C. Gabrielli, H. Perrot, F. Vicente, Electromechanical Phase Transition in Hexacyanometallate Nanostructure (Prussian Blue), Journal of the American Chemical Society. 129 (2007) 7121–7126. https://doi.org/10.1021/ja070895g.
[35] A. Arnau, T. Sogorb, Y. Jiménez, Circuit for continuous motional series resonant frequency and motional resistance monitoring of quartz crystal resonators by parallel capacitance compensation, Review of Scientific Instruments. 73 (7) (2002) 2724–2737, https://doi.org/10.1063/1.1484254.
[36] A. Cuenca, J. Agrisuelas, J.J. García-Jareño, F. Vicente, Oscillatory Changes of the Heterogeneous Reactive Layer Detected with the Motional Resistance during the Galvanostatic Deposition of Copper in Sulfuric Solution, Langmuir. 31 (46) (2015) 12664–12673, https://doi.org/10.1021/acs.langmuir.5b03694.
[37] C. Gabrielli, M. Keddam, N. Nadi, H. Perrot, ac Electrogravimetry on conducting polymers. Application to polyaniline, in: Workshop on the Electrochemistry of Electroactive Polymer FILMS (WEEPF97), Dourdan, France, 1997: pp. 2095–2103.
[38] C. Gabrielli, M. Keddam, N. Nadi, H. Perrot, Ions and solvent transport across conducting polymers investigated by ac electrogravimetry. Application to polyaniline, Journal of Electroanalytical Chemistry. 485 (2) (2000) 101–113, https://doi.org/10.1016/S0022-0728(00)00093-0.
[39] C. Gabrielli, J.J. García-Jareño, M. Keddam, H. Perrot, F. Vicente, Ac-Electrogravimetry Study of Electroactive Thin Films. I. Application to Prussian Blue, The Journal of Physical Chemistry B. 106 (12) (2002) 3182–3191, https://doi.org/10.1021/jp013924x.
[40] J. Agrisuelas, J.J. García-Jareño, D. Gimenez-Romero, F. Vicente, Innovative Combination of Three Alternating Current Relaxation Techniques: Electrical Charge, Mass, and Color Impedance Spectroscopy, Part I: The Tool, The Journal of Physical Chemistry C. 113 (19) (2009) 8430–8437, https://doi.org/10.1021/jp900823z.
[41] J. Agrisuelas, J.J. García-Jareño, D. Gimenez-Romero, F. Vicente, Innovative Combination of Three Alternating Current Relaxation Techniques: Electrical Charge, Mass, and Color Impedance Spectroscopy. Part II: Prussian Blue ⇆ Everitt's Salt Process, The Journal of Physical Chemistry C. 113 (19) (2009) 8438–8446, https://doi.org/10.1021/jp900824w.
[42] J. Gregori, J. Garcia-Jareno, F. Vicente, Determination of time dependence of passive layer on nickel from instantaneous mass/charge function F(dm/dQ) in competitive passivation/dissolution conditions, Electrochemistry Communications. 8 (5) (2006) 683–687, https://doi.org/10.1016/j.elecom.2006.03.006.
[43] J. Gregori, J.J. García-Jareño, D. Giménez-Romero, F. Vicente, Growth of passive layers on nickel during their voltammetric anodic dissolution in a weakly acid medium, Electrochimica Acta. 52 (2) (2006) 658–664, https://doi.org/10.1016/j.electacta.2006.05.051.
[44] D. Benito, C. Gabrielli, J.J. Garcı´a-Jareño, M. Keddam, H. Perrot, F. Vicente, Study by EQCM on the voltammetric electrogeneration of poly(neutral red). The effect of the pH and the nature of cations and anions on the electrochemistry of the films, Electrochimica Acta. 48 (27) (2003) 4039–4048, https://doi.org/10.1016/S0013-4686(03)00561-9.
[45] J.J. García-Jareño, D. Giménez-Romero, F. Vicente, C. Gabrielli, M. Keddam, H. Perrot, EIS and Ac-Electrogravimetry Study of PB Films in KCl, NaCl, and CsCl Aqueous Solutions, J. Phys. Chem. B. 107 (41) (2003) 11321–11330, https://doi.org/10.1021/jp035387h.
[46] L.i. Niu, C. Kvarnström, K. Fröberg, A. Ivaska, Electrochemically controlled surface morphology and crystallinity in poly(3,4-ethylenedioxythiophene) films, Synthetic Metals. 122 (2) (2001) 425–429, https://doi.org/10.1016/S0379-6779(00)00562-2.
[47] E. Poverenov, M. Li, A. Bitler, M. Bendikov, Major Effect of Electropolymerization Solvent on Morphology and Electrochromic Properties of PEDOT Films, Chem. Mater. 22 (13) (2010) 4019–4025, https://doi.org/10.1021/cm100561d.
[48] E. Tamburri, S. Orlanducci, F. Toschi, M.L. Terranova, D. Passeri, Growth mechanisms, morphology, and electroactivity of PEDOT layers produced by electrochemical routes in aqueous medium, Synthetic Metals. 159 (5-6) (2009) 406–414, https://doi.org/10.1016/j.synthmet.2008.10.014.
[49] N. Sakmeche, S. Aeiyach, J.-J. Aaron, M. Jouini, J.C. Lacroix, P.-C. Lacaze, Improvement of the Electrosynthesis and Physicochemical Properties of Poly(3,4-ethylenedioxythiophene) Using a Sodium Dodecyl Sulfate Micellar Aqueous Medium, Langmuir. 15 (7) (1999) 2566–2574, https://doi.org/10.1021/la980909j.
[50] S. Patra, K. Barai, N. Munichandraiah, Scanning electron microscopy studies of PEDOT prepared by various electrochemical routes, Synthetic Metals. 158 (10) (2008) 430–435, https://doi.org/10.1016/j.synthmet.2008.03.002.
[51] S. Bhandari, M. Deepa, S. Singh, G. Gupta, R. Kant, Redox behavior and optical response of nanostructured poly (3, 4-ethylenedioxythiophene) films grown in a camphorsulfonic acid based micellar solution, Electrochimica Acta. 53 (7) (2008) 3189–3199, https://doi.org/10.1016/j.electacta.2007.11.018.
[52] P. Manisankar, C. Vedhi, G. Selvanathan, H. Gurumallesh Prabu, Gurumallesh Prabu, Influence of surfactants on the electrochromic behavior of poly (3, 4-ethylenedioxythiophene), Journal of Applied Polymer Science. 104 (5) (2007) 3285–3291, https://doi.org/10.1002/app.25998.
[53] S. Zhang, J. Hou, R. Zhang, J. Xu, G. Nie, S. Pu, Electrochemical polymerization of 3, 4-ethylenedioxythiophene in aqueous solution containing N-dodecyl-β-d-maltoside, European Polymer Journal. 42 (1) (2006) 149–160, https://doi.org/10.1016/j.eurpolymj.2005.06.023.
[54] L. Pigani, A. Heras, Á. Colina, R. Seeber, J. López-Palacios, Electropolymerisation of 3,4-ethylenedioxythiophene in aqueous solutions, Electrochemistry Communications. 6 (11) (2004) 1192–1198, https://doi.org/10.1016/j.elecom.2004.09.021.
[55] M.F. Zainal, Y. Mohd, Characterization of PEDOT Films for Electrochromic Applications, Polymer-Plastics Technology and Engineering. 54 (3) (2015) 276–281, https://doi.org/10.1080/03602559.2014.977422.
[56] B. Zanfrognini, A. Colina, A. Heras, C. Zanardi, R. Seeber, J. López-Palacios, A UV–Visible/Raman spectroelectrochemical study of the stability of poly(3,4-ethylendioxythiophene) films, Polymer Degradation and Stability. 96 (12) (2011) 2112–2119, https://doi.org/10.1016/j.polymdegradstab.2011.09.017.
[57] J. MACDONALD, Impedance spectroscopy: Models, data fitting, and analysis, Solid State Ionics. 176 (25-28) (2005) 1961–1969, https://doi.org/10.1016/j.ssi.2004.05.035.
[58] J.J. García-Jareño, J.J. Navarro, A.F. Roig, H. Scholl, F. Vicente, Impedance analysis of Prussian Blue films deposited on ITO electrodes, Electrochimica Acta. 40 (9) (1995) 1113–1119, https://doi.org/10.1016/0013-4686(95)00017-9.
[59] E. Ventosa, J.L. Palacios, P.R. Unwin, Nucleation and growth of poly(3,4-ethylenedioxythiophene) thin films on highly oriented pyrolytic graphite (HOPG) electrodes, Electrochemistry Communications. 10 (11) (2008) 1752–1755, https://doi.org/10.1016/j.elecom.2008.09.003.
[60] M.J. González-Tejera, I. Carrillo Ramiro, I. Hernández-Fuentes, Nucleation and growth mechanism of polyfurane perchlorate doped films, Electrochimica Acta. 45 (12) (2000) 1973–1982, https://doi.org/10.1016/S0013-4686(99)00416-8.
[61] S. Sadki, P. Schottland, N. Brodie, G. Sabouraud, The mechanisms of pyrrole electropolymerization, Chemical Society Reviews. 29 (2000) 283–293, https://doi.org/10.1039/A807124A.
[62] E. Ventosa, A. Colina, A. Heras, A. Martínez, O. Orcajo, V. Ruiz, J. López-Palacios, Electrochemical, spectroscopic and electrogravimetric detection of oligomers occluded in electrochemically synthesized poly(3,4-ethylenedioxythiophene) films, Electrochimica Acta. 53 (12) (2008) 4219–4227, https://doi.org/10.1016/j.electacta.2007.12.064.
[63] E. Mitraka, M.J. Jafari, M. Vagin, X. Liu, M. Fahlman, T. Ederth, M. Berggren, M.P. Jonsson, X. Crispin, Oxygen-induced doping on reduced PEDOT, Journal of Materials Chemistry A. 5 (9) (2017) 4404–4412, https://doi.org/10.1039/C6TA10521A.
[64] B. Viswanathan, Chapter 13 – Supercapacitors, in: Energy Sources, Elsevier, Amsterdam, 2017, pp. 315–328, https://doi.org/10.1016/B978-0-444-56353-8.00013-7.
[65] S. Duluard, B. Ouvrard, A. Celik-Cochet, G. Campet, U. Posset, G. Schottner, M.-H. Delville, Comparison of PEDOT Films Obtained via Three Different Routes through

Spectroelectrochemistry and the Differential Cyclic Voltabsorptometry Method (DCVA), J. Phys. Chem. B. 114 (22) (2010) 7445–7451, https://doi.org/10.1021/jp9111712.
[66] L. Beverina, G.A. Pagani, M. Sassi, Multichromophoric electrochromic polymers: colour tuning of conjugated polymers through the side chain functionalization approach, Chem. Commun. 50 (41) (2014) 5413–5430, https://doi.org/10.1039/C4CC00163J.
[67] Q. Zhao, R. Jamal, L.i. Zhang, M. Wang, T. Abdiryim, The structure and properties of PEDOT synthesized by template-free solution method, Nanoscale Res Lett. 9 (1) (2014) 557, https://doi.org/10.1186/1556-276X-9-557.
[68] T. Nie, K. Zhang, J. Xu, L. Lu, L. Bai, A facile one-pot strategy for the electrochemical synthesis of poly(3,4-ethylenedioxythiophene)/Zirconia nanocomposite as an effective sensing platform for vitamins B2, B6 and C, Journal of Electroanalytical Chemistry. 717–718 (2014) 1–9, https://doi.org/10.1016/j.jelechem.2014.01.006.
[69] TaeYoung Kim, JongEun Kim, YunSang Kim, TaeHee Lee, WonJung Kim, K.S. Suh, Preparation and characterization of poly(3,4-ethylenedioxythiophene) (PEDOT) using partially sulfonated poly(styrene-butadiene-styrene) triblock copolymer as a polyelectrolyte, Current Applied Physics. 9 (1) (2009) 120–125, https://doi.org/10.1016/j.cap.2007.12.005.
[70] D. Hohnholz, A.G. MacDiarmid, D.M. Sarno, W.E. Jones, Jr., Uniform thin films of poly-3,4-ethylenedioxythiophene (PEDOT) prepared by in-situ deposition, Chem. Commun. (Camb.). (23) (2001) 2444–2445, https://doi.org/10.1039/b107130k.
[71] J. Agrisuelas, D. Giménez-Romero, J.J. García-Jareño, F. Vicente, Vis/NIR spectroelectrochemical analysis of poly-(Azure A) on ITO electrode, Electrochem. Commun. 8 (4) (2006) 549–553, https://doi.org/10.1016/j.elecom.2006.01.022.
[72] J. Agrisuelas, C. Gabrielli, J.J. García-Jareño, H. Perrot, F. Vicente, Kinetic and Mechanistic Aspects of a Poly(o-toluidine)-Modified Gold Electrode. 1. Simultaneous Cyclic Spectroelectrochemistry and Electrogravimetry Studies in H2SO4 Solutions, J. Phys. Chem. C. 116 (29) (2012) 15620–15629, https://doi.org/10.1021/jp303858q.
[73] J. Agrisuelas, C. Gabrielli, J.J. García-Jareño, H. Perrot, O. Sel, F. Vicente, Polymer dynamics in thin p-type conducting films investigated by ac-electrogravimetry. Kinetics aspects on anion exclusion, free solvent transfer, and conformational changes in poly(o-toluidine), Electrochim. Acta. 153 (2015) 33–43, https://doi.org/10.1016/j.electacta.2014.11.159.
[74] J. Agrisuelas, J.J. García-Jareño, D. Gimenez-Romero, F. Vicente, Innovative combination of three alternating current relaxation techniques: electrical charge, mass, and color impedance spectroscopy, Part I: the tool, The Journal of Physical Chemistry C. 113 (2009) 8430–8437, https://doi.org/10.1021/jp900823z.
[75] A. Ispas, R. Peipmann, A. Bund, I. Efimov, On the p-doping of PEDOT layers in various ionic liquids studied by EQCM and acoustic impedance, Electrochimica Acta. 54 (20) (2009) 4668–4675, https://doi.org/10.1016/j.electacta.2009.03.056.
[76] H. Liu, W. Zhou, X. Ma, S. Chen, S. Ming, K. Lin, B. Lu, J. Xu, Capacitive performance of electrodeposited PEDOS and a comparative study with PEDOT, Electrochimica Acta. 220 (2016) 340–346, https://doi.org/10.1016/j.electacta.2016.10.113.
[77] V. Lyutov, V. Gruia, I. Efimov, A. Bund, V. Tsakova, An acoustic impedance study of PEDOT layers obtained in aqueous solution, Electrochimica Acta. 190 (2016) 285–293, https://doi.org/10.1016/j.electacta.2015.12.177.
[78] R. Borjas, D.A. Buttry, Solvent swelling influences the electrochemical behavior and stability of thin films of nitrated poly (styrene), Journal of Electroanalytical Chemistry and Interfacial Electrochemistry. 280 (1) (1990) 73–90, https://doi.org/10.1016/0022-0728(90)87085-X.
[79] A.R. Hillman, M.A. Mohamoud, I. Efimov, Time-Temperature Superposition and the Controlling Role of Solvation in the Viscoelastic Properties of Polyaniline Thin Films, Anal. Chem. 83 (14) (2011) 5696–5707, https://doi.org/10.1021/ac200901d.